RESEARCH ARTICLE

Green composites based on volcanic red algae *Cyanidiales,* cellulose, and coffee waste biomass modified with magnetic nanoparticles for the removal of methylene blue

Paulina Pietrzyk[1] · Ewa Izabela Borowska[2] · Patrycja Hejduk[3] · Bruno Cury Camargo[4] · Magdalena Warczak[5] · Thu Phuong Nguyen[6] · Agnieszka Pregowska[1] · Marianna Gniadek[7] · Jacek Szczytko[4] · Sławomir Wilczewski[5] · Magdalena Osial[1]

Abstract
In this paper, green nanocomposites based on biomass and superparamagnetic nanoparticles were synthesized and used as adsorbents to remove methylene blue (MB) from water with magnetic separation. The adsorbents were synthesized through the wet co-precipitation technique, in which iron-oxide nanoparticles coated the cores based on coffee, cellulose, and red volcanic algae waste. The procedure resulted in materials that could be easily separated from aqueous solutions with magnets. The morphology and chemical composition of the nanocomposites were characterized by SEM, FT-IR, and XPS methods. The adsorption studies of MB removal with UV-vis spectrometry showed that the adsorption performance of the prepared materials strongly depended on their morphology and the type of the organic adsorbent. The adsorption studies presented the highest effectiveness in neutral pH with only a slight effect on ionic strength. The MB removal undergoes pseudo-second kinetics for all adsorbents. The maximal adsorption capacity for the coffee@Fe_3O_4–2, cellulose@Fe_3O_4–1, and algae@Fe_3O_4–1 is 38.23 mg g^{-1}, 41.61 mg g^{-1}, and 48.41 mg g^{-1}, respectively. The mechanism of MB adsorption follows the Langmuir model using coffee@Fe_3O_4 and cellulose@Fe_3O_4, while for algae@Fe_3O_4 the process fits to the Redlich-Peterson model. The removal efficiency analysis based on UV-vis adsorption spectra revealed that the adsorption effectiveness of the nanocomposites increased as follows: coffee@Fe_3O_4–2 > cellulose@Fe_3O_4–1 > algae@Fe_3O_4–1, demonstrating an MB removal efficiency of up to 90%.

Keywords Organic biomass waste · Magnetic nanoparticles · Water treatment · Adsorption · Eco-friendly composite · Green composite

Introduction

Water pollution is one of the most challenging environmental issues in the modern world (Rashid et al. 2021). Despite many commonly used water treatment techniques,

---

Responsible Editor: Tito Roberto Cadaval Jr

✉ Magdalena Osial
mosial@ippt.pan.pl

1 Institute of Fundamental Technological Research, Polish Academy of Sciences, Pawińskiego 5B, 02-106 Warsaw, Poland

2 The College of Inter-Faculty Individual Studies in Mathematics and Natural Sciences (MISMaP), University of Warsaw, Banacha 2C, 02-097 Warsaw, Poland

3 Faculty of Chemistry, University of Warsaw, Pasteura 1, 02-093 Warsaw, Poland

4 Institute of Experimental Physics, Faculty of Physics, University of Warsaw, Pasteura 5, 02-093 Warsaw, Poland

5 Faculty of Chemical Technology and Engineering, Bydgoszcz University of Science and Technology, Seminaryjna 3, 85-326 Bydgoszcz, Poland

6 Institute for Tropical Technology, Vietnam Academy of Science and Technology, 18 Hoang Quoc Viet, Cau Giay District, Hanoi 10000, Vietnam

7 Extremo Technologies, Klecińska 123, 54-413, Wrocław, Poland

innovative, cost-effective methods are still deeply needed. Effective wastewater treatment can be performed with many different techniques, including membrane separation (Li 2014; Wu et al. 2012), adsorption (Boi 2016; Nadour et al. 2019; Shao et al. 2008; Phuong et al. 2022; Oluse-gun et al. 2023a, b), photocatalytic oxidation (Rezaei et al. 2021), electrochemical methods (Alnajrani and Alsager 2020; Spaltro et al. 2020), biopolymer sorption (Zhou et al. 2016; Zhou et al. 2017a, b), photodegradation (Hussain et al. 2020; López Zavala and Espinoza Estrada 2016, Nagamine et al. 2020, Olusegun et al. 2023b), biosorption (Zhou et al. 2019), and biodegradation (Wang et al. 2020). Among them, adsorption-based processes are considered the most effective, also offering cost-effectiveness, simplicity of preparation, and high customizability (Rashed 2013). One of the most commonly used adsorbents is activated carbon. This material exhibits a high active surface area (Zhu et al. 2020; Mariana et al. 2021), enabling a responsive treatment of various types of chemicals in water, both at high and low concentrations. Despite being an outstanding adsorbent, activated carbon is not widely used in sewage treatment—mainly due to the high costs associated with its production and activation (Naganathan et al. 2021). Much effort has been put into finding equally efficient, yet cheaper alternatives. Nowadays, candidates for this role are natural materials called biosorbents, such as algae biomass, coffee grounds, or cellulose waste (Elgarahy et al. 2021). Coffee is the second most consumed beverage in the world (Begum et al. 2021), generating low-cost biomass that can be reused in many fields. It offers a highly porous structure that can effectively act as an adsorbent, while its sorption properties can be further improved by carbonization in strong acids, increasing the material's porosity (Conway 2021). In particular, activated carbon obtained from coffee residues can be a promising adsorbent for the removal of bisphenol A (Colantoni et al. 2021) and basic Toluidine Blue (Alves et al. 2019) from aqueous solutions. It has found use as a filtering agent for waste-, drinking- and contaminated waters (Gul et al. 2021). Moreover, it demonstrated the capability to trap heavy metals and toxic elements such as cadmium, lead, copper, and arsenic (Lafi et al. 2014; Azouaou et al. 2010; Kyzas 2012). Due to its effectiveness, it can be considered an attractive green and low-cost adsorbent material for the removal of diverse contaminants from water. Cellulose biomass is also widely used in water treatment (Nam et al. 2017; Chavan et al. 2016; Carpenter et al. 2015; Jiang et al. 2021) especially in heavy metals removal including lead, zinc, and cadmium (Li et al. 2021; Idress et al. 2021). Additionally, cellulose-based composites have controllable properties such as adsorption and pollutant degradation rates. Another biomaterial with promising properties in wastewater treatment is algae biomass (Wang et al. 2021; Leong et al. 2021). It can be used as an organic source of biomaterials in filters (Gupta

et al. 2021; Katam and Bhattacharyya 2021) and composites (Yadav et al. 2021; Eroglu et al. 2021). Among the many types of algae, microalgae are a low-cost and easily obtainable source of biomass with a large specific surface for the adsorption of different chemical compounds.

Regardless of the high effectiveness in water purification with biomass, it must be effectively removed from decontaminated solutions with filtration or be pre-prepared mechanically as a membrane. When associated with other well-established applications, nanotechnology holds great promise to address this issue in sustainable development. So far, coating biomass with magnetic particles for magnetic separation from water only with magnets can reduce wastewater costs. Besides providing magnetic properties, such an approach significantly improves the adsorption properties of the pristine compounds by enhancing their active surface areas (Arbab et al. 2021; Aragaw et al. 2021). One of the most promising materials for this application, offering a high surface area to volume ratio, non-cytotoxicity, fast kinetics, strong adsorption capacities, and photostability, is iron oxide (Sylvester et al. (2007); Pietrzyk et al. (2022); Olusegun et al. (2021)) making it possible to be applied in different fields, from water remediation to medical diagnostics and even vibration dissipation (Xu et al. 2012; Dave and Chopda 2014; Kaili et al. 2019; Gaweda et al. (2020); Żuk et al. 2021; Nieciecka et al. (2021); Osial et al. 2022). When used as a coat in core-shell composites, it improves the versatility and effectiveness of the adsorbent employed in wastewater treatment (Gutierrez et al. 2017), especially when it comes to the facile magnetic separation employing simple magnets or electromagnets and then reusing it in another treatment cycles (Sharma et al. 2018). Such an approach promotes sustainable development and perfectly matches the circular economy. The feasibility of Fe_3O_4-embedded filtering compounds has already been demonstrated in the literature. For example, in ref. (Taylor et al. 2012; Xie et al. 2014), a variety of adsorbent solutions based on iron oxide nanoparticles were reported. Magnetic nanocomposite adsorbents based on magnetite and clay have also been successfully applied for water purification in ref. (Alchouron et al. 2021) and photodegradation of organic pollutants (Liu et al. 2013). In addition, ref. (Na et al. 2021) shows iron oxide-biochar nanocomposites loaded with bacteria as a promising material for bioremediation in wastewater treatment. As the agricultural sector generates a tremendous amount of biomass waste, its effective management is a big issue. Therefore, its application in magnetic sorbents is not only an effective way to recycle agricultural waste but also shows it as a functional material that, thanks to the magnetic coat, simplifies the separation of the adsorbent after the effective treatment.

In this paper, methylene blue (MB) as a cationic dye with widespread use in textiles, was used as a model pollutant. Its disposal in waterways compromises the survival of aquatic

wildlife and humans feeding on it since MB contamination can lead to severe health problems (Hakami et al. 2021; Olusegun et al. 2021; Yang et al. 2020; Hameed et al. 2007). Its removal was performed with magnetic separation using biomass coated with iron oxide nanoparticles. Given this, we followed such a field, investigating the effectiveness of novel biowaste-based magnetic adsorbents in removing the model pollutant—methylene blue, from an aqueous solution, where the biomass was coffee, cellulose, and algae waste. The magnetic composite was characterized using scanning electron microscopy (SEM), Fourier transform infrared spectroscopy (FTIR), magnetometry, and X-ray photoelectron spectroscopy (XPS). The adsorption studies were performed using UV-vis spectrometry. Obtained results presented a promising applicability toward water purification.

Material and methods

Materials

The raw materials used as adsorbents in the present work were 100% arabica ground coffee obtained from Tchibo, microcrystalline cellulose with a purity $\geq 97\%$ from Merck S.A., and pelleted volcanic algae biomass of the *Cyanidiales* axenic strain (*Cyanidioschyzon merolae*, 10D, obtained from the Microbial Culture Collection at the National Institute of Environmental Studies in Japan), cultivated in low pH 1.5.

Materials used for the growth of magnetic nanoparticles were analytical-grade iron (III) chloride hexahydrate $FeCl_3 \cdot 6H_2O$ Aldrich ACS reagent 97% and iron (II) chloride tetrahydrate $FeCl_2 \cdot 4H_2O$ p.a. $\geq 99\%$. Both were supplied by Sigma-Aldrich co. Additionally, 25% ammonia solution NH_4OH was supplied by CHEMPUR, and ethanol 96% was supplied from POCH. Distilled water used during all steps of sample preparation was sourced from Merck's Milli-Q ultra-pure water filtering system and exhibited a resistivity of 18.2 M$\Omega \cdot$cm at 25 °C. Methylene blue (analytical grade) was purchased from WarChem Sp. z o.o., Poland.

Composite synthesis

In this work, core-shell magnetic nanoparticles were synthesized through a facile co-precipitation technique. Cores were adsorbents prepared from algae biomass, coffee waste, or cellulose, whereas shells were composed of iron oxide. The ratio between both of these components was chosen to yield nanoparticles with the highest possible efficiency in catching pollutants.

In total, three sets of samples were produced. They are described as follows: the first composite was based on coffee waste. Prior to use, ground coffee was leached in scalding water with a commercial coffee maker operating at a pressure of 14 bars, followed by air-drying on a hotplate at 90 °C for 2 h. The dried powder was stirred mechanically for 15 min in a 1:2 ethanol and water solution, filtered, and dried again at the same conditions.

To coat the coffee residue with iron oxide, 2 g of it was immersed in 10 mL of a solution containing 1.08 g of iron (III) chloride hexahydrate $FeCl_3 \cdot 6H_2O$ and 0.40 g of iron (II) chloride tetrahydrate $FeCl_2 \cdot 4H_2O$. The mixture was warmed up to 75 °C on a hotplate and stirred with a magnetic bar at a rate of about 1000 rpm to dissolve iron salts. To precipitate the iron oxide onto the organic core, the 25% ammonia solution was added dropwise until pH 10. The suspension was then stirred for 15 min at 75 °C. This process resulted in magnetite-covered ground coffee particles, with a ratio of 2 g of coffee per 570 mg $\pm$ 6 mg of Fe_3O_4 coat. The mass of iron oxide product on the organic core was estimated based on the weight of the dry powder mass. After the synthesis, the magnetic composite was collected at the bottom of the glass vial with a neodymium magnet and washed with deionized water until a neutral pH was achieved. The solid underwent air-drying on a hot plate at 75 °C for 1 h, followed by 90 °C for 1 h and subsequently 110 °C for 15 min. This drying method ensured slow evaporation of the water content, preventing steam-induced damage to the magnetic coating. The final product, labeled cofee@Fe_3O_4–1, was stored in a sealed glass vial prior to characterization.

Another batch of the cofee@Fe_3O_4 compound was also prepared with a different coffee: iron oxide ratio. It followed the same procedure outlined above but used 4 g of coffee residue (instead of 2 g). The resulting product, coffee@Fe_3O_4–2, had a lesser iron oxide coating onto the organic core than cofee@Fe_3O_4–1. The second composite was based on microcrystalline cellulose waste (cellulose@Fe_3O_4). The synthesis was performed following to same procedure outlined for cofee@Fe_3O_4, but by replacing the washed coffee with as-purchased microcrystalline cellulose. Therefore, to prepare cellulose@Fe_3O_4–1 and cellulose@Fe_3O_4–2 preparations, 2 g and 4 g of cellulose were used, respectively. As an effect, the ratio between the cellulose and iron oxide was about 4:1 (2 g of cellulose over 570 mg Fe_3O_4 coat)—cellulose@Fe_3O_4–1 and 8:1 (4 g of cellulose over 570 mg Fe_3O_4 coat)—cellulose@Fe_3O_4–2. The last composite was based on volcanic algae. Before synthesis, fresh algae were washed in water and centrifuged for several minutes, and then, the biomass was dried on a hot plate at 75 °C for 1 h. The dry biomass was subsequently fine-ground into a powder, where the same procedure of composite synthesis was performed. The ratio between the algae and iron oxide was about 4:1 (2 g of algae over 570 mg Fe_3O_4 coat)—algae@Fe_3O_4–1 and 8:1 (4 g of algae over 570 mg Fe_3O_4 coat)—algae@Fe_3O_4–2.

The biomass in sorbents was not carbonized—unlike most reports in the literature (Christou et al. 2018). This omission ensured a lower quantity of chemical refuse, thus reducing financial and environmental costs associated with the synthesis process.

Methods

Before morphology characterization, all composites (before and after coating with Fe_3O_4) were dispersed in ethanol at the ratio of 5 mg·mL^{-1}, drop-casted onto a flat surface, and allowed to dry in a vacuum overnight. Their morphologies were obtained with a scanning electron microscope (SEM)—FE-SEM Merlin (Zeiss, Oberkohen, Germany) equipped with a Gemini II column. The chemical composition of the samples was measured with X-ray photoelectron spectroscopy (XPS) using a PHI 5000 VersaProbe (ULVAC-PHI) spectrometer with monochromatic Al Kα radiation (hν = 1486.6 eV). XPS spectra were collected with a hemispherical analyzer at a pass energy of 23.5 eV and 0.1 eV resolution. Magnetic properties were investigated with a quantum design magnetic property measurement system (MPMS XL-7), on magnetic fields below 7 T and in the temperature range 2 K < T < 300 K. UV-vis spectrometry was employed to evaluate chemical concentrations in aqueous solutions. Absorption spectra were recorded using a Perkin Elmer Lambda 35 spectrophotometer.

Results and discussion

Morphological analysis

The morphology of the composites was investigated with scanning electron microscopy. Samples prepared using 2 g of waste and 570 mg of iron oxide (X@Fe$_3$O$_4$–1, X = coffee, cellulose, or algae) presented morphologies composed of large surfaces with smooth contours. Meanwhile, samples prepared by using 4 g of biomass over 570 mg of iron oxide (X@Fe$_3$O$_4$–2) revealed non-homogeneous morphology and differences in the samples with an increase in the waste mass. As can be seen in Fig. 1a for coffee@Fe$_3$O$_4$–1, the magnetic oxide uniformly covered the whole surface of the coffee grains. This was denoted by rough agglutinated spherical structures, as shown in Fig. 1b. The composite coffee@Fe$_3$O$_4$–2 exhibited a less homogeneous iron oxide coating. Instead, they revealed a rich structure composed of nanometric magnetic nanostructures adhered to the adsorbent (see Fig. 1c, d).

SEM micrographs obtained for cellulose@Fe$_3$O$_4$ samples are presented in Fig. 2. Results revealed significantly different morphologies in comparison with bare cores. In the composite cellulose@Fe$_3$O$_4$–1, the iron oxide formed a smooth film over the organic adsorbent, with few irregularities (see Fig. 2a, b). Particles synthesized with larger cellulose; iron oxide ratios exhibited less homogeneous coatings, see Fig. 2c, d for cellulose@Fe$_3$O$_4$–2. As can be seen, iron

Fig. 1 Morphology of coffee@Fe$_3$O$_4$ composite synthesized from solutions containing **a**, **b** 2 g and **c**, **d** 4 g starting quantities of coffee. The orange ring in the left column corresponds to the region magnified in the right column
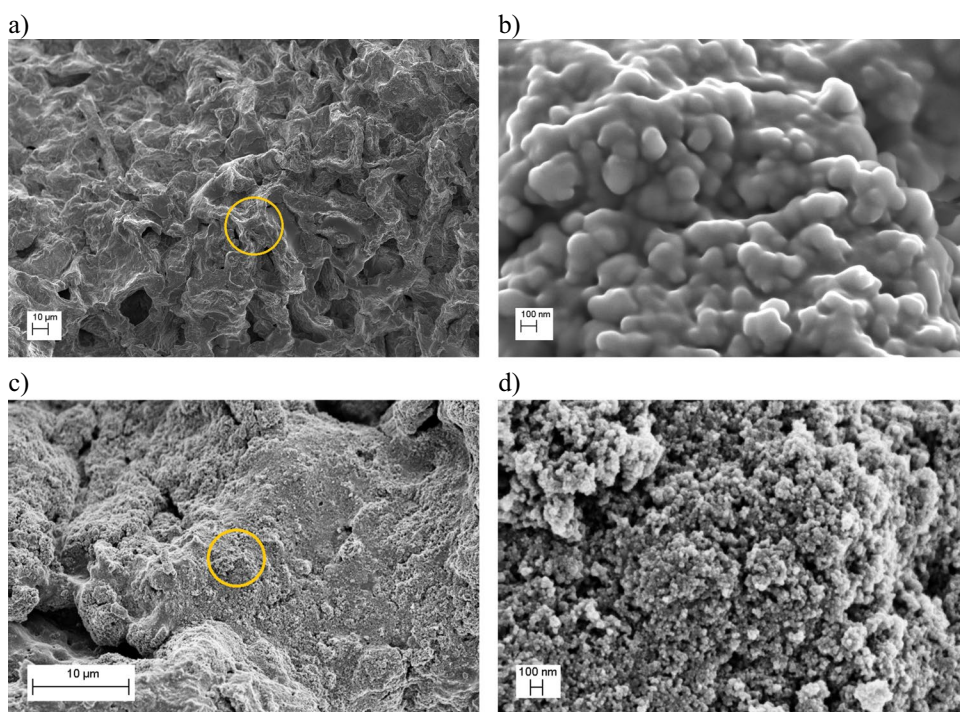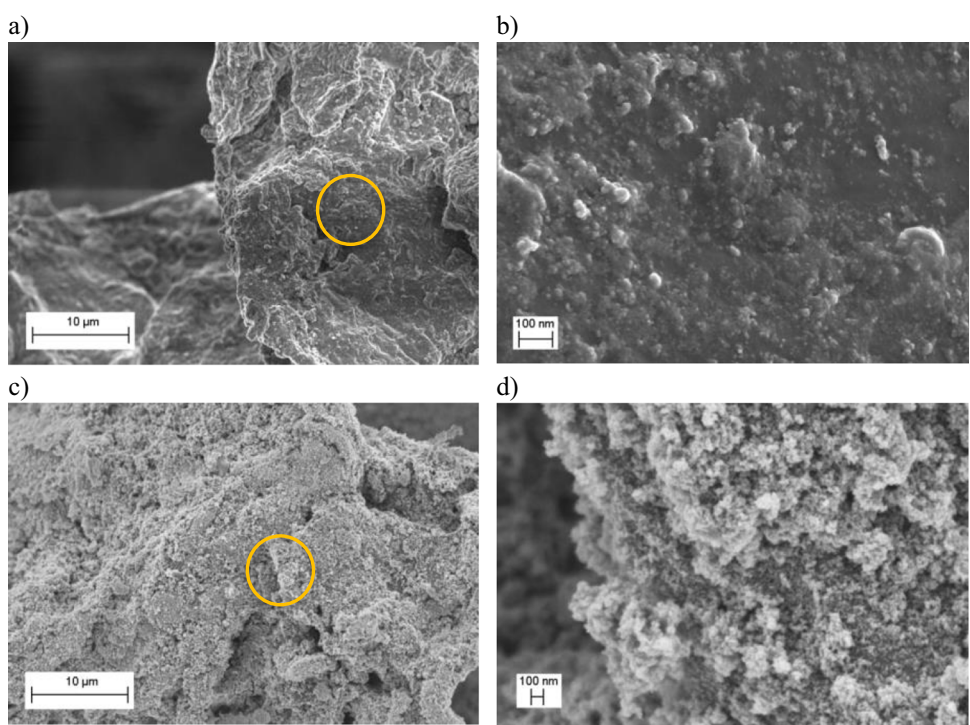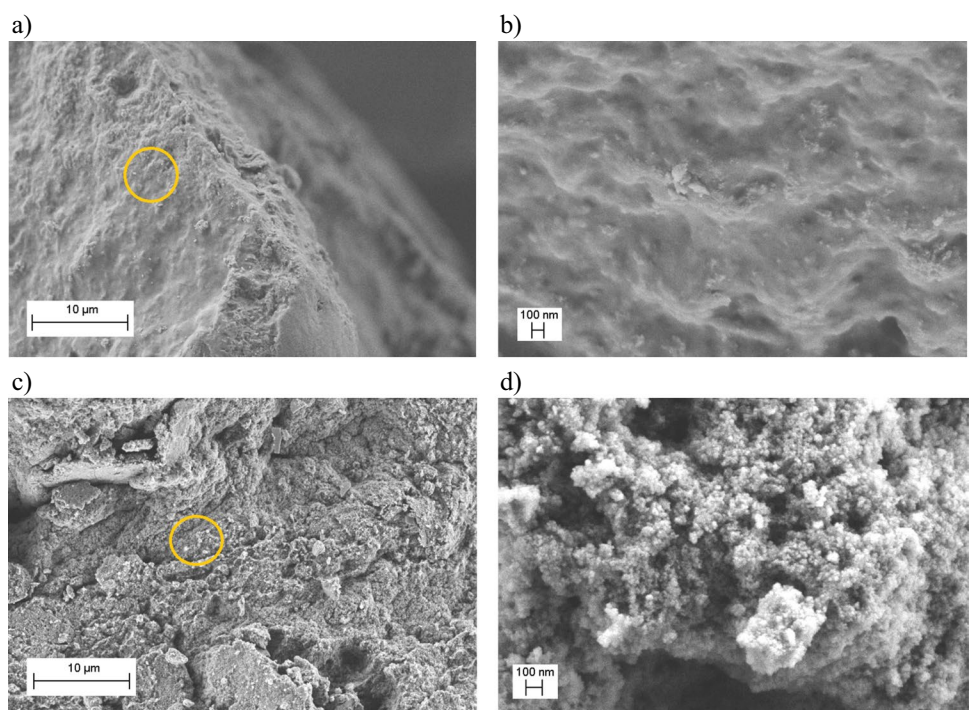
Fig. 2 Morphology of cellulose@Fe$_3$O$_4$ composite synthesized from solutions containing **a**, **b** 2 g and **c**, **d** 4 g starting quantities of cellulose. The orange ring in the left column corresponds to the region magnified in the right column

oxide formed irregular clusters of nanoparticles across the adsorbent's surface.

In the composite algae@Fe$_3$O$_4$–1 (Fig. 3a, b), iron oxide formed a smooth layer on the algae surface. This can be caused by the morphology of the microalgae, as this raw adsorbent had a much smaller size in comparison to the remaining ones. For algae@Fe$_3$O$_4$–2 (Fig. 3c, d), on the other hand, the overall features of the iron oxide coating were similar to those found on the other composites. Namely, clusters of nanoparticles with typical sizes below

Fig. 3 Morphology of algae@Fe$_3$O$_4$ composite synthesized from solutions containing **a**, **b** 2 g and **c**, **d** 4 g starting quantities of algae. The orange ring in the left column corresponds to the region magnified in the right column

100 nm formed, increasing the composite's specific surface and improving its potential as a pollutant adsorbent.

Based on the morphology studies, it is seen that the adsorbent offering the largest surface is coffee@Fe$_3$O$_4$-2, cellulose@Fe$_3$O$_4$-1, and algae@Fe$_3$O$_4$-1, so these samples were used for the adsorption studies.

FT-IR and XPS chemical composition studies

After the morphological studies, composites were characterized through Fourier transformed infrared spectroscopy (FT-IR). This allowed the identification of the most important functional groups included in our specimens confirming the chemical composition of the samples. Results are shown in Fig. 4. They revealed that all iron oxide-coated adsorbents presented similar spectra, composed by a superposition of characteristic peaks of Fe–O lattices and an attenuated background due to the sample core. In it, the peak at about
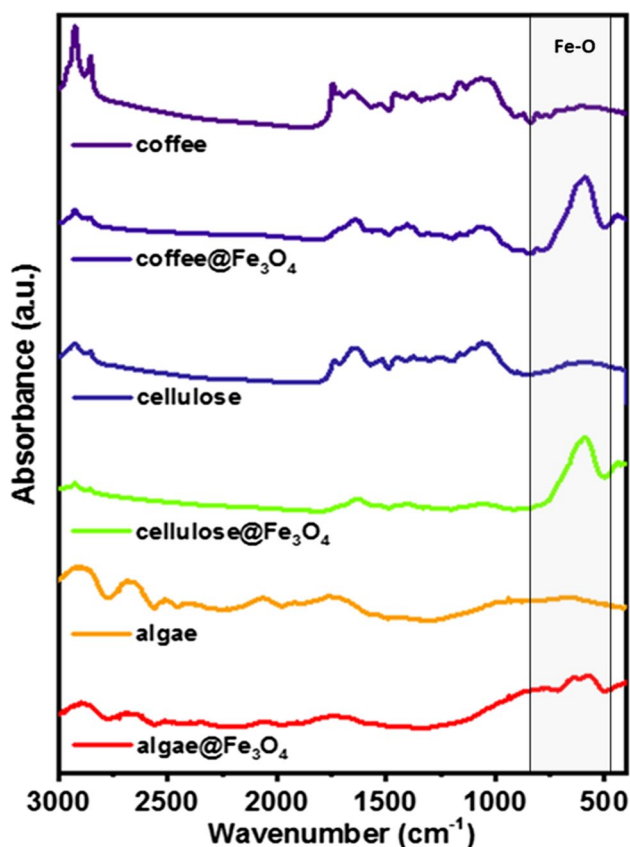

Fig. 4 FT-IR spectra for adsorbent cores and their composites. Curves correspond to (from top to bottom): coffee, coffee@Fe$_3$O$_4$–2 cellulose, cellulose@Fe$_3$O$_4$–1, algae, and algea@Fe$_3$O$_4$–1 composite

2925 cm^{-1} corresponds to the C-H stretching of aliphatic or even aromatic acids, whereas the one at 1745 cm^{-1} can be assigned to the carboxylic groups. The peak at 1713 cm^{-1} stands for either aliphatic acids or ketones, and the one at 1654 cm^{-1} can relate to the C-O stretching and cis C-C bonding (Christou et al. 2018). The presence of the carboxylic group (COO-) is confirmed by a peak at 1527 cm^{-1}. Wide peaks appearing at the range 2500–3000 cm^{-1} are attributed to the O-H valence vibrations of carboxylic acids with hydrogen bridges and can be seen in the spectra of algae. The peaks below 650 cm^{-1} can be ascribed to the Fe-O vibrations in the SPIONs' lattice (Lesiak et al. 2019).

As X-ray Photoelectron Spectroscopy (XPS) can provide information on the elemental composition of the adsorbent surface and its chemical valence state, it was used complementary to the FT-IR analysis. The spectra presented in Fig. 5a show the chemical binding states of the iron oxide nanoparticles. The survey spectra for all three composites were similar and did not depend on the iron oxide: adsorbent ratio during sample synthesis. Peaks corresponding to C 1 s are ascribed to the organic core, while Fe 2p corresponds to the iron oxide. Due to the latter being located in the NP shell, the Fe peak intensity is much higher than that of carbon. Figure 5b shows a representative XPS measurement of the C 1 s band of the organic absorbents, achieved by probing the coffee-based material. The obtained spectrum is broad and can be deconvoluted into three peaks, associated with different chemical bonds of carbon. Among them, particular peaks marked in different colors in the spectrum can be distinguished. The peak centered at 287.2 eV can be assigned to the C–C or C-H bonds. Meanwhile, the ones centered at 289.3 eV and 291.0 eV can be ascribed to C-N and O = C–OH, respectively (Chickos 2018). Figure 5c shows an XPS spectrum of Fe 2p, revealing two peaks at 713.0 eV and 727.0 eV. These binding energies can be deconvoluted into peaks that correspond to Fe-O bonds characteristic of Fe$_3$O$_4$ which is made of FeO·Fe$_2$O$_3$. The spectrum for Fe is composed of Fe^{2+} and Fe^{3+}, where the valence state increases with the binding energy (Biesinger et al. 2011; Wilson and Langell 2014). The satellite peaks for both valent states are also presented within the spectrum. Results for iron compounds were identical to those presented, which confirmed the formation of iron oxide onto the organic core and will not be shown here. Lastly, the spectrum presented in Fig. 5d is associated with the O 1 s orbital, where the main peak corresponds to the oxygen, that is, the iron oxide lattice. The lower peak can be ascribed to the presence of oxygen in the organic core, relating to the bonds that are also visible at C 1 s (Lesiak et al. 2019), see Fig. 5a.

Fig. 5 a X-ray photoelectron spectroscopy measurements of the composites (from top to bottom): coffee@Fe_3O_4–2, cellulose @Fe_3O_4–1, and algae@Fe_3O_4–1. XPS spectra of bands correspond to **b** C1s, **c** Fe2p, and **d** O1s. The particular bands are described in the text
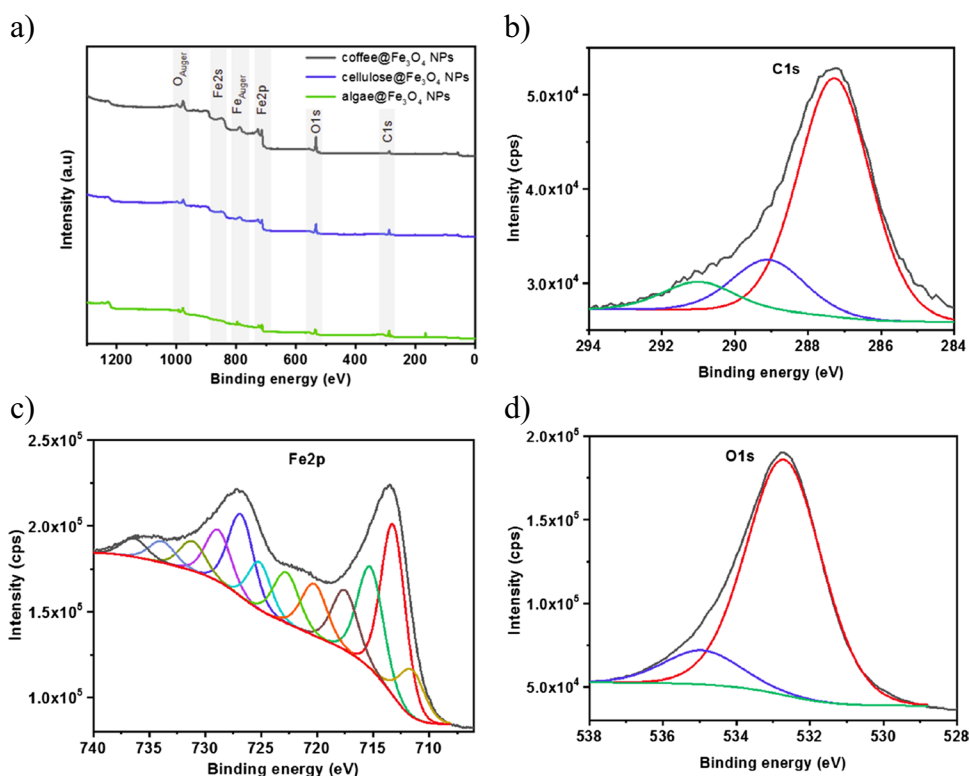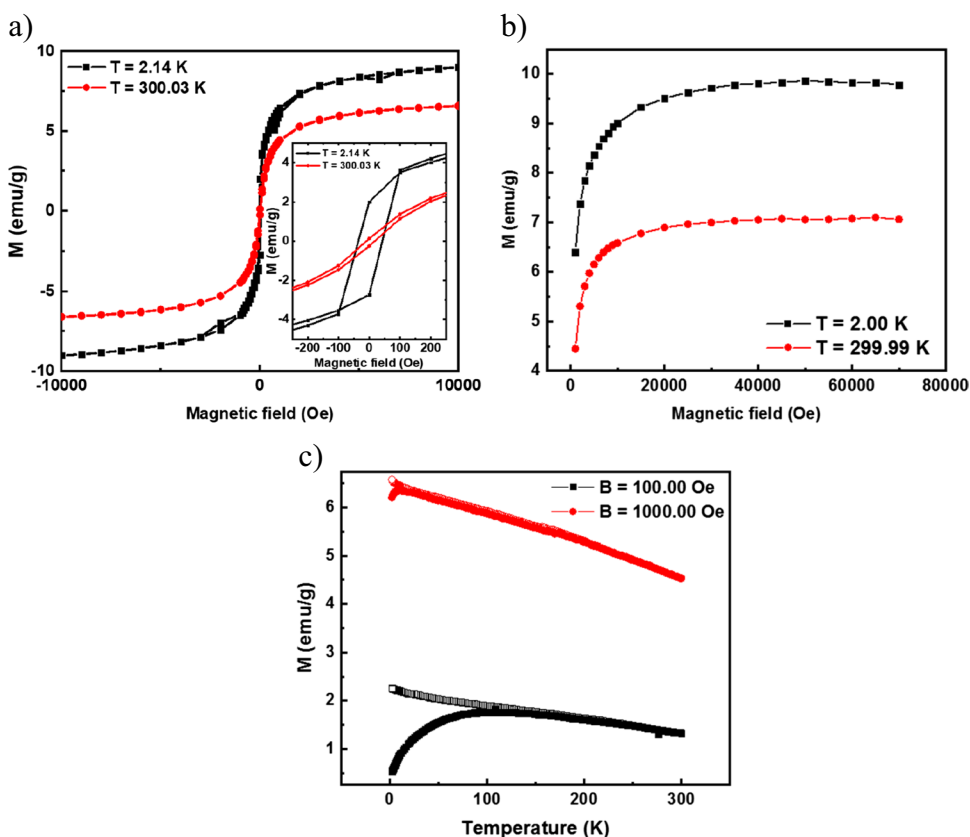

Fig. 6 a M(H) hysteresis loops obtained for coffee@Fe_3O_4-2 at T = 2 K (black squares) and T = 300 K (red circles). No discernible coercive field is observable; **b** M(H) measurements up to the highest available field. Saturation occurs above B ~ 2000 Oe and **c** M(T) measurements on coffee@Fe_3O_4. Data was obtained in the ZFC (filled symbols) and FCC (empty symbols) regimes

Investigation of magnetic properties

Magnetic properties of biomass-based nanocomposite were determined by magnetic moment measurements in the temperature interval 2 K < T < 300 K and magnetic fields H up to 70 kOe. Figure 6a, b shows that the M(H) curves revealed a saturation magnetization at T = 300 K around 7 emu·g^{-1}, which increased with the reduction of temperature up to 9.8 emu·g^{-1} at T = 2 K. The inset presented in Fig. 6a reveals very low coercivity of the prepared sample. As the magnetic separation of the proposed materials is an important feature in the presented studies, a deep investigation of the material was performed, including the temperature dependence of magnetization following zero-field-cooled (ZFC) and field-cooled on cooling (FCC) protocols. In the former, the sample was cooled at zero magnetic fields and measured upon warming, whereas in the latter, the measurements occur while cooling the material. Results revealed a paramagnetic, glassy-like behavior that did not obey the Curie-Weiss law up to 300 K (Coey 2009). A hysteresis between the ZFC and FCC curves was present in measurements performed at H = 100 Oe but was almost completely suppressed for fields as small as 1 kOe. The presence of a maximum on M(T, H = 100 Oe) curves at T ~ 100 K could indicate that the compound is composed of a disordered array of magnetic centers with a collective blocking temperature of around 100 K (Fig. 6c).

Despite presenting many inferior properties to pristine magnetite (Kemp et al. 2016), the magnetism of the composites studied here suffices for their application toward the magnetic separation of pollutants.

UV-vis studies

The effectiveness of the composites in adsorbing methylene blue (MB) pollutants from an aqueous solution was investigated through UV-vis spectrometry. Measurements were performed as a function of the composite amount in solution and the time of exposure to pollutants. The largest effectiveness was achieved for the composites coffee@Fe$_3$O$_4$–2, cellulose@Fe$_3$O$_4$–1, and algae@Fe$_3$O$_4$–1. UV-vis spectra were recorded in the wavelength range from 700 to 200 nm in a quartz cuvette.

First, the studies were performed in function of adsorbent mass, where 1, 2, 5, 10, and 20 mg were added to 20 mL of 10 ppm (40 μmol) MB solution with a contact time of about 10 min. Figure 6a–c shows dependence on the used mass of the composites in the adsorption, where the highest % efficiency was obtained for 20 mg of adsorbent. Therefore, such a mass was chosen for the determination of the optimal conditions in the subsequent studies. The time applied for analysis was 10 min. The spectra were normalized to an

Fig. 7 UV-vis spectra of adsorption MB, where the used mass is in the range 1–20 mg for composites: **a** coffee@Fe$_3$O$_4$, **b** cellulose@Fe$_3$O$_4$, and **c** algae@Fe$_3$O$_4$
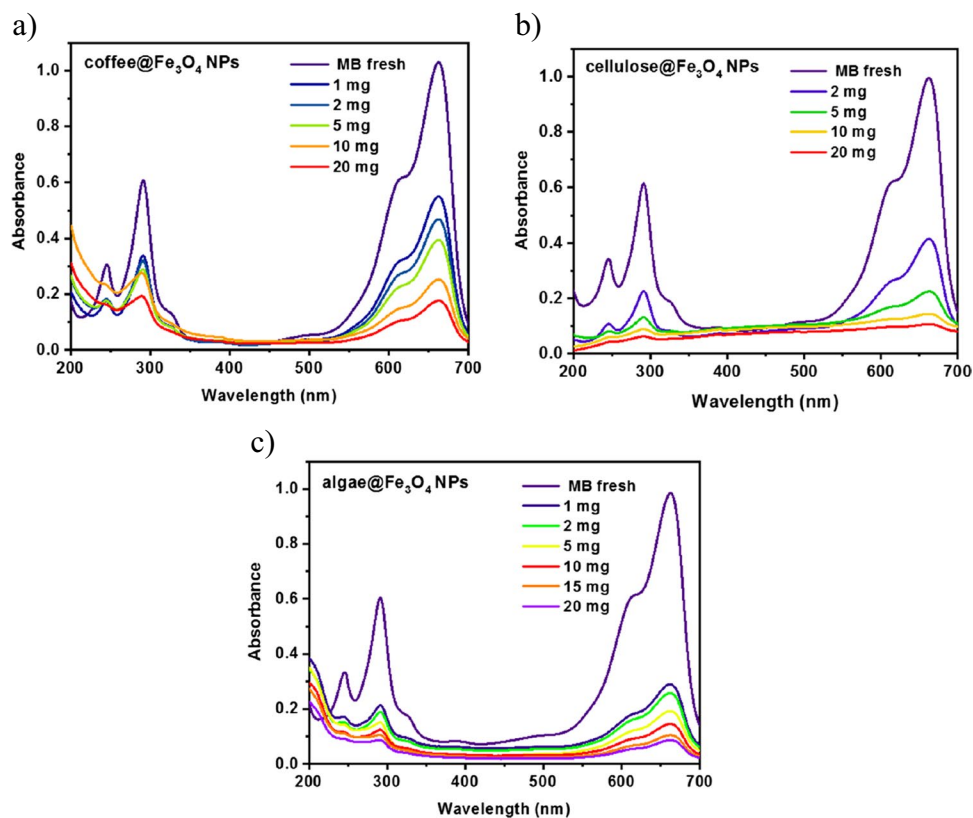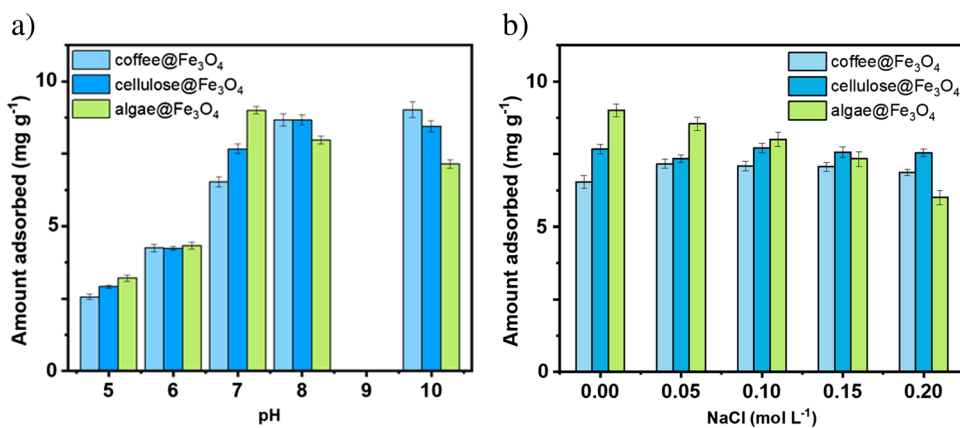
**Fig. 8** MB amount adsorbed by composited in the function of **a** pH and **b** ionic strength

absorbance equal to 1 (Fig. 7).pH effect and ionic strength are some of the most important variables, which influence pollution adsorption because the wastewater can have different pH and salinity. Figure 8a shows the amount of adsorbent with different pH range from 5 to 10, where the amount of adsorbent was calculated by using Eq. 1:

$$Q = \frac{(C_0 - C_t) \times V}{m} \tag{1}$$

where C_0 is the initial concentration of dye ($mg \cdot g^{-1}$), C_t is the concentration of dye in time ($mg \cdot g^{-1}$), V is the volume (L), m is the mass of adsorbent (g), and Q is the amount of adsorbent ($mg \cdot g^{-1}$).

The removal of MB by composites increased with the rise of pH value. The highest value was obtained in pH 7 for algae but pH 8 for other composites, which were applied for kinetic studies because of the smallest differences between materials. The subsequent measurements were performed with different concentrations of NaCl in pH 7. Figure 8b shows the increase of ionic strength prompted by to decrease

Fig. 9 **a** Efficiency of adsorption as a function of time, **b** adsorption data modeled using kinetic Lagergren's pseudo-first-order, and **c** adsorption data modeled using kinetic McKay and Ho's pseudo-second-order law
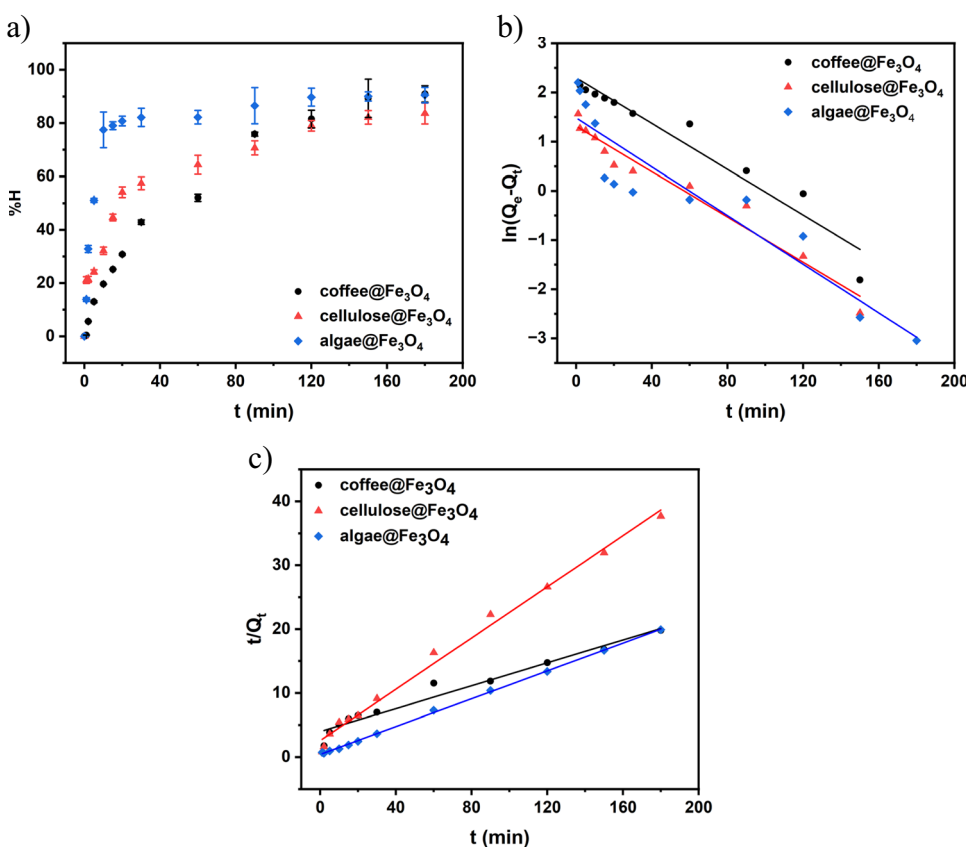
in the amount of adsorbent, especially for algae but composite based on cellulose and coffee displayed similar effectiveness in the MB adsorption process.

Figure 9a shows the adsorption of MB removal efficiency as a function of time. The process was guided by 180 min; within this time, composites made of algae and coffee, %H efficiency overstepped the 90%, were observed, but for cellulose composite, the removal of dye was reduced compared to other composites. The concentration of dye after the adsorption process was calculated from Eq. 2:

$$\%H = (C_0 - C_t/C_0) \times 100\%, \tag{2}$$

where C_t is the MB concentration at time t (mg·L^{-1}), and C_0 is the initial MB concentration (mg·L^{-1}).

Next, the measurements were performed in function of contact time. Based on the obtained results, it can be seen that the 20 min is sufficient to reach over 80% adsorption efficiency %H for algae@Fe$_3$O$_4$-1, while the elongation of the contact time leads to even higher effectiveness of about 90%, see Fig. 9a. For the coffee waste-based adsorbent, similar effect is achieved after 180 min exposition. (Banat et al. 2003) shows a similar effect, where MB rapidly attaches the adsorbent attaches surface, which is followed by a much slower process associated with the rough surface of iron oxide NPs (Banat et al. 2003). The cellulose-based adsorbent also requires longer contact time than the coffee-based one, while H% values are lower than those of the other composites. Based on the measured removal of the pollutant in contact time, order of the adsorption process has been determined, so in the following studies, MB was treated for 180 min with the proposed magnetic adsorbents.

Adsorption kinetics was characterized by tracking the intensity of spectrophotometric absorption peak 662 nm as a function of time. The kinetics of the pseudo-first adsorption process of MB molecule to a surface can be described through the following Eq. 3:

$$\ln(Q_e - Q_t) = lnQ_e - k_1 t \tag{3}$$

where Q_t stands for the amount of adsorbed material per unit mass of adsorbent at a time t, whereas Q_e corresponds to its value at equilibrium (Franca et al. 2009). The parameter $k_{1,2}$ (e.g. k_2) is known as the rate constant for pseudo kinetic order adsorption.

For pseudo-second-order kinetic, it follows Eq. 4:

$$t/Q_t = 1/k_2 Q_e{}^2 + t/Q_e \tag{4}$$

To determine the kinetics, the values of correlation coefficients R^2 were compared. Figure 9b shows the fitting to the pseudo-first-model kinetics, while Fig. 9c demonstrates the fitting to the pseudo-second-order. Parameters from the fitting linear equation and kinetic parameters have been presented in Table 1. Based on the obtained results, it is seen that the adsorption process follows pseudo-second kinetic order for all composites. The Q_e values for cellulose and algae composites were similar due to the equilibrium conditions; however, for coffee@Fe$_3$O$_4$, these results differ, suggesting that such material requires a longer time to achieve equilibrium during MB adsorption.

As the effectiveness of MR removal differs for particular sorbents, the adsorption isotherms were subsequently measured, providing information about the adsorbent equilibrium performance. The isotherms were estimated for the different concentrations of model pollutants. The initial concentration was changed within the range of 20–180 mg L^{-1} for MB in pH 7 for algae but for coffee and cellulose in pH 8. Experimental data were fitted into the non-linear equations of Langmuir (Eq. 5), Freundlich (Eq. 6), and Redlich-Peterson (Eq. 7) adsorption isotherms (Fig. 9).

$$Q_e = \frac{Q_{max}K_L C_e}{1 + K_L C_e} \tag{5}$$

$$Q_e = K_F C_e{}^{1/n} \tag{6}$$

$$Q_e = \frac{K_{RP} C_e}{1 + a_{RP} C_e{}^g} \tag{7}$$

where C_e stands for the equilibrium concentration (mg L^{-1}), Q_e is the equilibrium adsorbed (mg g^{-1}), Q_{max} is the maximum adsorption capacity (mg g^{-1}), K_L is Langmuir equilibrium constant (L mg^{-1}), K_F is the Freundlich constant (mg g^{-1} (mg L^{-1})$^{-1/nF}$), n_F is the dimensionless exponent of Freundlich, where K_{RP} (L g^{-1}) and a_{RP} (mg L^{-1})$^{-g}$, g is an R-P dimensionless parameter (Wu et al. 2010).

Figure 10 shows the non-linear fitting of the adsorption isotherms for the MB removal for all adsorbents. The

Table 1 Parameters from linear fitting kinetic orders

Composite	$k_1 \cdot 10^{-3}$ (min^{-1})	Q_{exp} (mg g^{-1})	R^2 I kinetic order	$k_2 \cdot 10^{-3}$ (g mg^{-1} min^{-1})	Q_{exp} (mg g^{-1})	R^2 II kinetic order	$Q_{cal.}$ (mg g^{-1})
Coffee@Fe$_3$O$_4$	23.26	9.9577	0.9323	1.9972	9.0300	0.9591	11.1907
Cellulose@Fe$_3$O$_4$	23.03	3.7113	0.9538	15.477	4.7777	0.9914	4.9945
Algae@Fe$_3$O$_4$	24.77	4.3915	0.8601	27.838	9.0492	0.9993	9.2072

Fig. 10 Adsorption isotherms for the MB removal with a) coffee@Fe$_3$O$_4$-2, b) cellulose@Fe$_3$O$_4$-1, and c) algae@Fe$_3$O$_4$-1
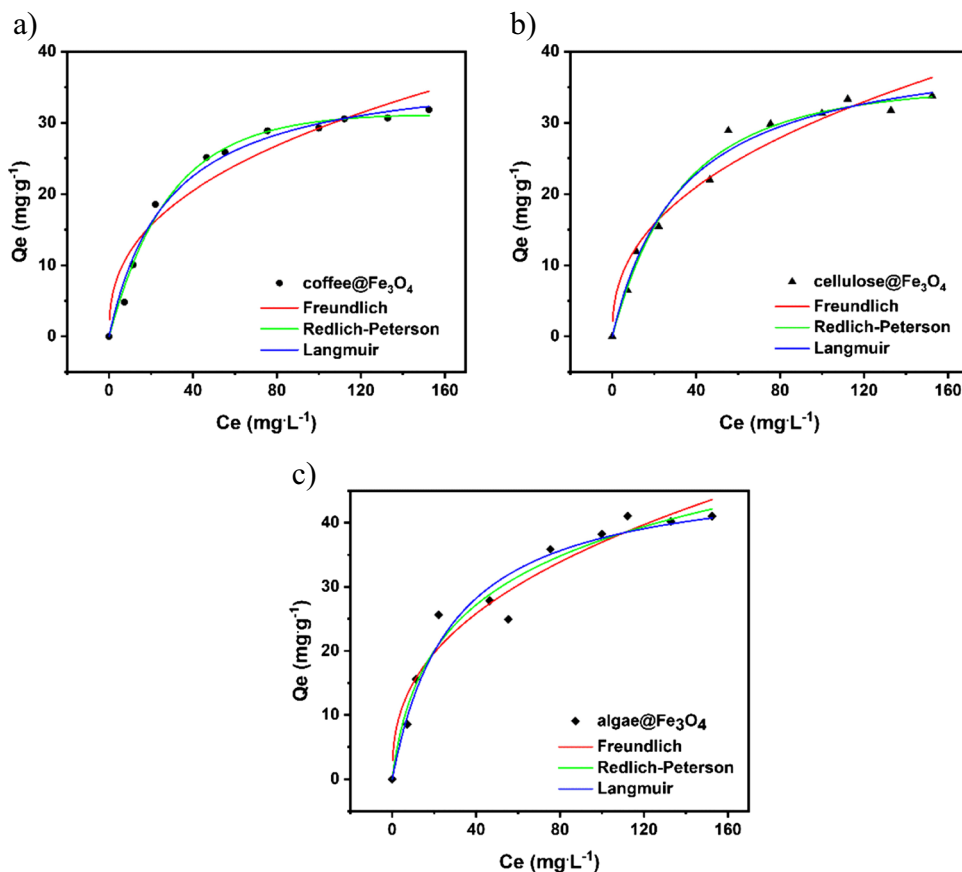
Table 2 Isotherms parameters for the MB removal

Isotherms parameters	Composites		
	Coffee@Fe$_3$O$_4$	Cellulose@Fe$_3$O$_4$	Algae@Fe$_3$O$_4$
Langmuir			
Q_{max}	38.2301	41.6712	48.1113
K_L	0.0357	0.0301	0.0347
R^2	0.9855	0.9822	0.9518
Freundlich			
K_F	4.8621	4.6044	6.0743
N	2.5678	2.4329	2.5502
R^2	0.8866	0.9190	0.9128
Redlich-Peterson			
K_{RP}	1.0557	1.0722	2.7074
a_{RP}	0.0089	0.0136	0.1520
G	1.2241	1.1239	0.8072
R^2	0.9907	0.9814	0.9531

correlation coefficient R^2 values for all adsorbents are the highest for Langmuir and Redlich-Peterson models. However, the value of g factor is higher than 1 for coffee and cellulose-based adsorbents which excludes the Redlich-Peterson model. Therefore, it can be assumed that the cellulose@Fe$_3$O$_4$ and coffee@Fe$_3$O$_4$ follow the Langmuir model.

At the same time, the g factor for the algae@Fe$_3$O$_4$ is lower than 1, suggesting the best fitting to the Redlich-Peterson model, see Table 2, presenting the obtained parameters of isotherms. The adsorption capacity of MB on the surface of used composites: algae@Fe$_3$O$_4$ > cellulose@Fe$_3$O$_4$ > coffee@Fe$_3$O$_4$.

Table 3 has shown compared values of obtained adsorption capacity with other nanoparticles and composites. Obtained values of Q_{max} are comparable with some materials demonstrated in the literature.

Conclusions

In summary, composites based on organic cores and iron oxide shells can be synthesized by the co-precipitation method as an effective way for biomass waste reuse. The obtained magnetic sorbents can be easily used for the removal of dyes from aqueous solutions, which are considered emerging aqueous contaminants and have a potentially harmful impact on living organisms. As a proof of concept, in this paper, green composites based on biomass waste were proposed for the biosorption and removal of methylene blue from water—a potential pollutant widely applied in the chemical and textile industries. The iron-oxide coating ensured a subsequent simple removal of the

Table 3 Compared obtain adsorption capacity with others materials

The material used for MB adsorption	Q_{max} [mg g^{-1}]	References
Activated carbon prepared from *Delonix regia* pods	24.00	(Ho et al. 2009)
Activated carbon prepared from wood apple shell	36.90	(Malarvizhi and Sulochana 2008)
Spent coffee grounds	18.73	(Franca et al. 2009)
Composite material made of algae	74.00	(Vilar et al. 2007)
Kaolin	52.76	(Mouni et al. 2018)
Raw ball clay	34.652	(Auta and Hameed 2012)
Graphene-like carbon material	20.0	(Lingamdinne et al. 2018a)
Graphitic carbon-like material	38.75	(Lingamdinne et al. 2018b)
Magnetic fly ash	9.27	(Ahmed et al. 2022)
Expanded graphite/Fe_3O_4	78.06	(Wu et al. 2021)
Magnetic chitosan nanocomposite	20.408	(Rahmi and Irfan 2019)
Bio-silica	52.60	(Olusegun et al. 2021)
8%-S-Monolith	10.80	(Kaya-Özkiper et al. 2022)
Coffee@Fe_3O_4	38.23	This work
Cellulose@Fe_3O_4	41.61	This work
Algae@Fe_3O_4	48.41	This work

exhausted filtering media from the solution by magnetic means. All composites presented in this study (coffee@ Fe_3O_4, cellulose@ Fe_3O_4, and algae@ Fe_3O_4) were successfully used as supportive materials for the removal of contaminants from water with magnetic sorbent. However, their effectiveness was dictated by the ratio between the core adsorbent and its iron oxide coating. It was found that the degree of activity of our specimens was strictly related to the type of organic adsorbent and the morphology of the composite. For coffee@Fe_3O_4, the highest effectiveness was achieved by an iron oxide-to-core ratio of 8:1 (coffee@Fe_3O_4–2), whereas for the remaining composites, the ratio was 4:1 (cellulose@ Fe_3O_4–1 and algae@ Fe_3O_4–1). The adsorption studies showed that the highest effectiveness of the MB removal was near neutral pH, while the presence of salt in the solution slightly affected the process. Kinetic studies showed a pseudo-second-order adsorption process for all compounds. Despite a higher core-shell ratio needed for effective MB removal from solution, the coffee@Fe_3O_4–1 and algae@Fe_3O_4–1 removed compounds at a higher yield, thus showing greater promise as composites for wastewater treatment. This may be due to the large iron oxide-specific surfaces achieved on these adsorbent cores. The Langmuir isotherm was found suitable to explain the MB adsorption process using coffee@Fe_3O_4 and cellulose@Fe_3O_4, while for algae@Fe_3O_4 the best model is Redlich-Peterson. The maximal adsorption capacity for the sorbents is as follows: 38.23 mg g^{-1} for coffee@Fe_3O_4, 41.61 mg g^{-1} for cellulose@Fe_3O_4, and 48.41 mg g^{-1} for algae@Fe_3O_4, respectively. The broad access to waste organic biomass, the use of magnetic nanocomposites based on natural biosorbents,

and the employment of iron oxide to remove organic pollutants from aquatic systems seem to be an economically and technologically practical solution to solving a major global issue. We expect our results to encourage further research activity on the subject, including the synthesis of magnetic core/shell composites with other, locally available, green core materials for wastewater treatment.

Authors contributions Conceptualization, methodology, supervision—Magdalena Osial; formal analysis, and data curation—Patrycja Hejduk, Thu Phuong Nguyen, Marianna Gniadek, Paulina Pietrzyk, and Sławomir Wilczewski; investigation—Patrycja Hejduk, Magdalena Warczak, Bruno Camargo, Thu Phuong Nguyen, Paulina Pietrzyk, Agnieszka Pregowska, and Magdalena Osial; original draft writing—Bruno Camargo, Agnieszka Pregowska, and Magdalena Osial; resources—Ewa Borowska, Jacek Szczytko, and Magdalena Osial. All authors have read, edited, and approved the final manuscript.

Data availability The datasets used and/or analyzed during the current study are available from the corresponding author on a reasonable request.

Declarations

Ethical approval Not applicable

Consent to participate Not applicable

Consent to publish Not applicable

Competing interests The authors declare no competing interests.

References

Ahmed FS, Alsaffar MA, AbdulRazak AA (2022) One-step synthesis of magnetic fly ash composites for methylene blue removal: batch and column study. Environ Sci Pollut Res. https://doi.org/10.1007/s11356-022-23491-x

Alchouron J, Navarathna C, Rodrigo PM, Snyder A, Chludil HD, Vega AS, Bosi G, Perez F, Mohan D, Pittman CU Jr, Mlsna TE (2021) Household arsenic contaminated water treatment employing iron oxide/bamboo biochar composite: an approach to technology transfer. J Colloid Interface Sci 587:767–779

Alnajrani MN, Alsager OA (2020) Removal of Antibiotics from water by polymer of intrinsic microporosity: isotherms, kinetics, thermodynamics, and adsorption Mechanism. Sci Rep 10:794

Alves ACF, Antero RVP, de Oliveira SB, Ojala SA, Scalize PS (2019) Activated carbon produced from waste coffee grounds for an effective removal of bisphenol-A in aqueous medium. Environ Sci Pollut Res Int 26(24):24850–24862

Aragaw TA, Bogale FM, Aragaw BA (2021) Iron-based nanoparticles in wastewater treatment: a review on synthesis methods, applications, and removal mechanisms. J Saudi Chem Soc 5(8):101280

Arbab A, Tufail S, Rehmat U, Pingfan Z, Manlin G, Muhammad O, Zhiqiang T, YuKui R (2021) Review on recent progress in magnetic nanoparticles: synthesis, characterization, and diverse applications. Front Chem 9:548

Auta M, Hameed BH (2012) Modified mesoporous clay adsorbent for adsorption isotherm and kinetics of methylene blue. Chem Eng J 198–199:219–227

Azouaou N, Sadaoui Z, Djaafri A, Mokaddem H (2010) Adsorption of cadmium from aqueous solution onto untreated coffee grounds: equilibrium, kinetics and thermodynamics. J Hazard Mater 184:126–134

Banat F, Al-Asheh S, Al-Makhadmeh L (2003) Evaluation of the use of raw and activated date pits as potential adsorbents for dye containing waters. Process Biochem 39(2):193–202

Begum S, Yuhana NY, Saleh NM, Kamarudin NHN, Sulong AB (2021) Review of chitosan composite as a heavy metal adsorbent: Material preparation and properties. Carbohyd Polym 259:117613

Biesinger MC, Payne BP, Grosvenor AP, Lau LWM, GersonSmart ARRSC (2011) Resolving surface chemical states in XPS analysis of first row transition metals, oxides and hydroxides: Cr, Mn, Fe, Co and Ni. Appl Surf Sci 257(7):2717–2730

Boi C (2016) Removal of antibiotics from wastewaters by membrane operations. In: Drioli E, Giorno L (eds) Encyclopedia of membranes. Springer, Berlin, Heidelberg. 1724–1725

Carpenter AW, de Lannoy CF, Wiesner MR (2015) Cellulose nanomaterials in water treatment technologies. Environ Sci Technol 49(9):5277–5287

Chavan AA, Pinto J, Liakos I, Bayer IS, Lauciello S, Athanassiou A, Fragouli D (2016) Spent coffee bioelastomeric composite foams for the removal of Pb^{2+} and Hg^{2+} from water. ACS Sustain Chem Eng 4:5495–5502

Chickos JS (2018) Heat of sublimation data: in NIST Chemistry Web-Book, NIST Standard Reference Database Number 69, Linstrom PJ and Mallard WG (Eds.) National Institute of Standards and Technology, Gaithersburg MD, 20899 (retrieved Sept. 10, 2021)

Christou C, Agapiou A, Kokkinofta R (2018) Use of FTIR spectroscopy and chemometrics for the classification of carobs origin. J Adv Res 10:1–8

Coey J (2009) Magnetism and magnetic materials. Cambridge University Press, Cambridge

Colantoni A, Paris E, Bianchini L, Ferri S, Marcantonio V, Carnevale M, Palma A, Civitarese V, Gallucci F (2021) Spent coffee ground characterization, pelletization test and emissions assessment in the combustion process. Sci Rep 11:5119

Conway J (2021) https://www.statista.com/statistics/292595/global-coffee-consumption/ (available on 18.02.2023)

Dave PN, Chopda LV (2014) Application of iron oxide nanomaterials for the removal of heavy metals. J Nanotechnol 2014(398569

Elgarahy AM, Elwakeel KZ, Mohammad SH, Elshoubaky GA (2021) A critical review of biosorption of dyes, heavy metals and metalloids from wastewater as an efficient and green process. Cleaner Engineering and Technology 4:100209

Eroglu E, Brown MM, Lou X (2021) 15 - Application of electrospun composite materials for algal bioprocesses, In Dong Y, Baji A, Ramakrishna S (Eds) Woodhead Publishing Series in Composites Science and Engineering, Electrospun Polymers and Composites, Woodhead Publishing 449–469. https://doi.org/10.1016/B978-0-12-819611-3.00015-7

Franca AS, Oliveira LS, Ferreira ME (2009) Kinetics and equilibrium studies of methylene blue adsorption by spent coffee grounds. Desalination 249(1):267–272

Gaweda W, Osial M, Żuk M, Pękała M, Bilewicz A, Krysiński P (2020) Lanthanide-doped SPIONs bioconjugation with trastuzumab for potential multimodal anticancer activity and magnetic hyperthermia. Nanomaterials 10:288

Gul A, Khaligh NG, Julkapli NM (2021) Surface modification of carbon-based nanoadsorbents for the advanced wastewater treatment. J Mol Struct 1235:130148

Gupta S, Nayak A, Roy C, Yadav AK (2021) An algal assisted constructed wetland-microbial fuel cell integrated with sand filter for efficient wastewater treatment and electricity production. Chemosphere 263:128132

Gutierrez AM, Dziubla TD, Hilt JZ (2017) Recent advances on iron oxide magnetic nanoparticles as sorbents of organic pollutants in water and wastewater treatment. Rev Environ Health 32(1–2):111–117

Hakami AAH, Wabaidur SM, Khan MA, AlOthman AZ, Siddiqui MR (2021) Extraction procedures and analytical methods for the determination of methylene blue, rhodamine B and crystal violet - an overview. Curr Anal Chem 17(5):708–728

Hameed BH, Ahmad AL, Latiff KN (2007) Adsorption of basic dye (methylene blue) onto activated carbon prepared from rattan sawdust. Dyes Pigm 75:143–149

Ho YS, Malarvizhi R, Sulochana N (2009) Equilibrium isotherm studies of methylene blue adsorption onto activated carbon

prepared from Delonix regia pods. J Ennvironm Prot Sci 3:111–116

Hussain S, Ullah Khan S, Gul S (2020) 17 - Electrochemical treatment of antibiotics in wastewater. In Hashmi MZ (Ed.) Antibiotics and antimicrobial resistance genes. Environmental occurrence and treatment technologies, Springer International Publishing, 355–394

Idress H, Zaidi SZJ, Sabir A, Shafiq M, Khan RU, Harito C, Hassan S, Walsh FC (2021) Cellulose acetate based complexation-NF membranes for the removal of Pb(II) from waste water. Sci Rep 11:1806

Jiang Z, Ho SH, Wang X, Li Y, Wang C (2021) Application of biodegradable cellulose-based biomass materials in wastewater treatment. Environ Pollut 290:118087

Kaili Q, Weijun T, Jie B, Liang W, Jing Z, Zhaoyang D, Xiaoxi G (2019) Application of magnetic adsorbents based on iron oxide nanoparticles for oil spill remediation: a review. J Taiwan Inst Chem Eng 97:227–236

Katam K, Bhattacharyya D (2021) Improving the performance of activated sludge process with integrated algal biofilm for domestic wastewater treatment: system behavior during the start-up phase. Bioresour Technol Rep 13:100618

Kaya-Özkiper K, Uzun A, Soyer-Uzun S (2022) Tuning adsorption, structure and compressive strength of sepiolite- and metakaolin-based alkali activated monoliths for methylene blue removal from waste water. Surf Interfaces 33:102110

Kemp S, Fergurson R, Khandar A, Krishnan K (2016) Monodisperse magnetite nanoparticles with nearly ideal saturation magnetization RSC. Advances 6:77452–77464

Kyzas GZ (2012) Commercial coffee wastes as materials for adsorption of heavy metals from aqueous solutions. Materials 5(10):1826–1840

Lafi R, ben Fradj A, Hafiane A, Hameed BH (2014) Coffee waste as potential adsorbent for the removal of basic dyes from aqueous solution. Korean J Chem Eng 31(2198):2206

Leong YK, Huang CY, Chang JS (2021) Pollution prevention and waste phycoremediation by algal-based wastewater treatment technologies: the applications of high-rate algal ponds (HRAPs) and algal turf scrubber (ATS). J Environ Manage 296:113193

Lesiak B, Rangam N, Jiricek P, Gordeev I, Tóth J, Kövér L, Mohai M, Borowicz P (2019) Surface study of Fe3O4 nanoparticles functionalized with biocompatible adsorbed molecules. Front Chem 7:642

Li WC (2014) Occurrence, sources, and fate of pharmaceuticals in aquatic environment and soil. Environ Pollut 187:193–201

Li A, Gong Y, Zhao D, Dang A, Lin Z (2021) Enhanced removal of zinc and cadmium from water using carboxymethyl cellulose-bridged chlorapatite nanoparticles. Chemosphere 263:128038

Lingamdinne LP, Singh J, Choi JS, Chang YY, Yang JK, Karri RR, Koduru JR (2018a) Multivariate modeling via artificial neural network applied to enhance methylene blue sorption using graphene-like carbon material prepared from edible sugar. J Mol Liq 265:416–427

Lingamdinne LP, Choi JS, Yang JK, Chang YY, Koduru JR, Singh J (2018b) Adsorptive removal of selected anionic and cationic dyes by using graphitic carbon material prepared from edible sugar: a study of kinetics and isotherms. Acta Chim Slov 65(3):599–610

Liu X, Wang M, Zhang S, Pan B (2013) Application potential of carbon nanotubes in water treatment: a review. J Environ Sci 25(7):1263–1280

López Zavala MÁ, Espinoza Estrada E (2016) Degradation of acetaminophen and its transformation products in aqueous solutions by using an electrochemical oxidation cell with stainless steel electrodes. Water 8(9):383

Malarvizhi R, Sulochana N (2008) Sorption Isotherm and Kinetic Studies of Methylene Blue Uptakeonto Activated Carbon Prepared from Wood Apple Shell. J Enironm Prot Sci 2:40–46

Mariana M, Mulana F, Juniar L, Fathira D, Safitri R, Muchtar S, Bilad MR, Shariff AHM, Huda N (2021) Development of biosorbent derived from the endocarp waste of Gayo coffee for lead removal in liquid wastewater—effects of chemical activators. Sustainability 13:3050

Mouni L, Belkhiri L, Bollinger JC, Bouzaza A, Assadi A, Tirri A, Dahmoune F, Madani K, Remini H (2018) Removal of Methylene Blue from aqueous solutions by adsorption on Kaolin: Kinetic and equilibrium studies. Appl Clay Sci 153:38–45. https://doi.org/10.1016/j.clay.2017.11.034

Na S, Lee S, Youn S (2021) Experiment on activated carbon manufactured from waste coffee grounds on the compressive strength of cement mortars. Symmetry 13:619

Nadour M, Boukraa F, Benaboura A (2019) Removal of diclofenac, paracetamol and metronidazole using a carbon-polymeric membrane. J Environ Chem Eng 7(3):103080

Nagamine M, Osial M, Widera-Kalinowska J, Jackowska K, Krysinski P (2020) Photosensitive thin films based on drop cast and Langmuir-Blodgett hydrophilic and hydrophobic CdS nanoparticles. Nanomaterials 10:2437

Naganathan KK, Faizal ANM, Zaini MAA, Ali A (2021) Adsorptive removal of bisphenol a from aqueous solution using activated carbon from coffee residue. Materials Today: Proceedings 47(6):1307–1312

Nam G, Kim MS, Lee N, Choi YH, Ahn JW (2017) An environmentally benign approach for as (V) Absorption from wastewater using untreated coffee grounds—preliminary results. Water 9:867

Nieciecka D, Celej J, Żuk M, Majkowska-Pilip A, Żelechowska-Matysiak K, Lis A, Osial M (2021) Hybrid system for local drug delivery and magnetic hyperthermia based on SPIONs loaded with doxorubicin and epirubicin. Pharmaceutics 13:480

Olusegun SJ, Freitas ETF, Lara LRS, Mohallem NDS (2021) Synergistic effect of a spinel ferrite on the adsorption capacity of nano bio-silica for the removal of methylene blue. Environ Technol 42(14):2163–2176

Olusegun SJ, Osial M, Souza TGZ, Krajewski M, Rodrigues GLS, Pękała M, Krysinski P (2023a) Comparative characteristics and enhanced removal of tetracycline and ceftriaxone by Fe3O4-lignin and Fe3O4-carbon-based lignin: mechanism, thermodynamic evaluation, and DFT calculation. J Mol Liq 371:21075

Olusegun SJ, Souza TGF, Souza GDO, Osial M, Mohallem NDS, Ciminelli VST, Krysinski P (2023b) Iron-based materials for the adsorption and photocatalytic degradation of pharmaceutical drugs: a comprehensive review of the mechanism pathway. J Water Process Eng 51:103457

Osial M, Nowicki M, Klejman E, Frąś L (2022) Investigation of the well-dispersed magnetorheological oil-based suspension with superparamagnetic nanoparticles using modified split Hopkinson pressure bar. Rheol Acta 61:111–122

Phuong NT, Thom NT, Nam PT, Van Trang N, Huong TTT, Hai DT, Thu LP, Osial M, Thanh DTM (2022) Co2+ and Cr3+ ions removal from wastewater by using nanostructural hydroxyapatite. VJCH 60:135–147

Pietrzyk P, Phuong NT, Olusegun SJ, Hong Nam N, Thanh DTM, Giersig M, Krysiński P, Osial M (2022) Titan yellow and Congo red removal with superparamagnetic iron-oxide-based nanoparticles doped with zinc. Magnetochemistry 8:91

Rahmi I, Irfan M (2019) Methylene blue removal from water using H2SO4 crosslinked magnetic chitosan nanocomposite beads. Microchem J 1444:397–402

Rashed MN (2013) Adsorption technique for a removal of organic pollutants from water and wastewater. In Organic pollutants

– monitoring, risk and treatment, intechOpen. 167–194. https://doi.org/10.5772/54048

Rashid R, Shafiq I, Akhter P, Iqbal MJ, Hussain M (2021) A state-of-the-art review on wastewater treatment techniques: the effectiveness of adsorption method. Environ Sci Pollut Res 28:9050–9066

Rezaei SS, Kakavandi B, Noorisepehr M, Isari AA, Zabih S, Bashardoust P (2021) Photocatalytic oxidation of tetracycline by magnetic carbon-supported TiO$_2$ nanoparticles catalyzed peroxydisulfate: performance, synergy and reaction mechanism studies. Sep Purif Technol 258(1):117936

Shao J, Fang X, He Y, Jin Q (2008) Emergency membrane contactor based absorption system for ammonia leaks in water treatment plants. J Environ Sci 20(10):1189–1194

Sharma M, Kalita P, Senapati K, Garg A (2018) Study of magnetic materials for removal of water pollutants. IntechOpen. https://doi.org/10.5772/intechopen.75700

Spaltro A, Pila MN, Colasurdo DD, Noseda Grau E, Roman G, Simonetti S, Ruiz DL (2020) Removal of paracetamol from aqueous solution by activated carbon and silica. Experimental and computational study. J Contam Hydrol 236:103739

Sylvester P, Westerhoff P, Möller T, Badruzzaman M, Boyd O (2007) A hybrid sorbent utilizing nanoparticles of hydrous iron oxide for arsenic removal from drinking water. Environ Eng Sci 24(1):104–112

Taylor EN, Kummer KM, Durmus NG, Leuba K, Tarquinio KM, Webster TJ (2012) superparamagnetic iron oxide nanoparticles (spion) for the treatment of antibiotic-resistant biofilms. Small 8:3016–3027

Vilar VJP, Botelho CMS, Boaventura RAR (2007) Methylene blue adsorption by algal biomass based materials: Biosorbents characterization and process behaviour Journal of Hazardous Materials 147(1–2):120–132. https://doi.org/10.1016/j.jhazmat.2006.12.055

Wang H, Zhang J, Yuan X, Jiang L, Xia Q, Chen H (2020) Photocatalytic removal of antibiotics from natural water matrices and swine wastewater via Cu(I) coordinately polymeric carbon nitride framework. Chem Eng J 39:123638

Wang J, Zhang G, Qiao S, Zhou J (2021) Magnetic Fe0/iron oxide-coated diatomite as a highly efficient adsorbent for recovering phosphorus from water. Chem Eng J 412:128696

Wilson D, Langell MA (2014) XPS analysis of oleylamine/oleic acid capped Fe$_3$O$_4$ nanoparticles as a function of temperature. Appl Surf Sci 303:6–13

Wu FC, Liu BL, Wu KT, Tseng RL (2010) A new linear form analysis of Redlich-Peterson isotherm equation for the adsorption of dyes. Chem Eng J 162(1):21–27

Wu S, Zhang L, Chen J (2012) Paracetamol in the environment and its degradation by microorganisms. Appl Microbiol Biotechnol 96(4):875–884

Wu K-H, Huang W-C, Hung W-C, Tsai C-W (2021) Modified expanded graphite/Fe3O4 composite as an adsorbent of methylene blue: adsorption kinetics and isotherms. Mater Sci Eng, B 266:15068

Xie J, Wang Z, Wu D, Kong H (2014) Synthesis and properties of zeolite/hydrated iron oxide composite from coal fly ash as efficient adsorbent to simultaneously retain cationic and anionic pollutants from water. Fuel 116:71–76

Xu P, Zeng GM, Huang DL, Feng CL, Hu S, Zhao MH, Lai C, Wei Z, Huang C, Xie GX, Liu ZF (2012) Use of iron oxide nanomaterials in wastewater treatment: a review. Sci Total Environ 424:1–10

Yadav G, Shanmugam S, Sivaramakrishnan R, Kumar D, Mathimani T, Brindhadevi K, Pugazhendhi A, Rajendran K (2021) Mechanism and challenges behind algae as a wastewater treatment choice for bioenergy production and beyond. Fuel 285:19093

Yang CW, Liu C, Chang BV (2020) Biodegradation of amoxicillin, tetracyclines and sulfonamides in wastewater sludge. Water 12(8):2147

Zhou Y, Zhang Z, Zhang J, Xia S (2016) Understanding key constituents and feature of the biopolymer in activated sludge responsible for binding heavy metals. Chem Eng J 304:527–532

Zhou Y, Xia S, Nguyen BT, Zhang J, Zhang Z (2017a) Interactions between metal ions and the biopolymer in activated sludge: quantification and effects of system pH value. Front Environ Sci Eng 11:7

Zhou Y, Xia S, Zhang J, Nguyen BT, Zhang Z (2017b) Insight into the influences of pH value on Pb(II) removal by the biopolymer extracted from activated sludge. Chem Eng J 308:1098–1104

Zhou Y, Marcus AK, Straka L, Eustance E, Jung Y, Lai S, Xia S, Rittmann BE (2019) Uptake of phosphate by Synechocystis sp. PCC 6803 in dark conditions: removal driving force and modeling. Chemosphere 218:147–156

Zhu Y, Wang W, Yu H, Wang A (2020) Preparation of porous adsorbent via Pickering emulsion template for water treatment: a review. J Environ Sci 88:217–236

Żuk M, Gawęda W, Majkowska-Pilip A, Osial M, Wolski M, Bilewicz A, Krysiński P (2021) Hybrid radiobioconjugated superparamagnetic iron oxide-based nanoparticles for multimodal cancer therapy. Pharmaceutics 13:1843